PB82227398

UMTA-MA-06-0025-82-1
DOT-TSC-UMTA-81-69

Limiting Forces on Transit Trucks in Steady-State Curving

R. Greif
H. Weinstock

U.S. Department of Transportation
Research and Special Programs Administration
Transportation Systems Center
Cambridge MA 02138

May 1982
Interim Report

U.S. Department of Transportation
Urban Mass Transportation Administration

Office of Technical Assistance
Office of Systems Engineering
Washington DC 20590

Technical Report Documentation Page

1. Report No. UMTA-MA-06-0025-82-1	2. Government Accession No.	3. Recipient's Catalog No. PB82 227398
4. Title and Subtitle: Limiting Forces on Transit Trucks in Steady-State Curving.		5. Report Date: May 1982
		6. Performing Organization Code: DTS-743
7. Author(s): R. Greif, and H. Weinstock		8. Performing Organization Report No.: DOT-TSC-UMTA-81-69
9. Performing Organization Name and Address: U.S. Department of Transportation, Research & Special Programs Administration, Transportation Systems Center, Cambridge, Massachusetts 02142		10. Work Unit No. (TRAIS): MA-06-0025
		11. Contract or Grant No.
12. Sponsoring Agency Name and Address: **U.S. Department of Transportation, Urban Mass Transportation Administration, 400 Seventh Street, S.W. Washington, D. C. 20590**		13. Type of Report and Period Covered: Interim Report Oct. 1981-Sept. 1981
		14. Sponsoring Agency Code: URT-10
15. Supplementary Notes		

16. Abstract

The Wheel/Rail Dynamics Project of the Urban Rail Systems Program is directed toward the development of technical data that can be applied to improve performance specifications for transit car trucks and components to permit reductions in maintenance costs and wheel/rail noise while providing acceptable ride quality and safety. To define the potential improvement achievable in curving performance of transit trucks, a limiting value analysis is performed on current and candidate truck configurations to establish bounds on the expected curving performance. Results of this analysis are presented in this document.

This study develops conservative bounds on wheel/rail forces and flange forces for several types of rigid and flexible trucks in steady-state curving conditions. The approximate analysis presented provides closed-form relations for estimating forces, truck angle of attack, creep force saturation and sliding conditions as a function of truck geometry and track parameters. The wheel profiles are modeled by conical wheel treads with vertical wheel flanges. Limiting case transit truck configurations are anlyzed to provide comparison of the benefits achievable in curving performance from modification of truck geometry. These limiting configurations include: ideal rigid truck; ideal parallelogramming truck; ideal radial (self-steering) truck; ideal guided steering truck; and compensating guided steering truck. Results of this report can be used in the design and specification of trucks for transit or railroad operations to estimate the wheel/rail interaction forces and slip behavior produced during curve negotiations.

17. Key Words: Truck/Car Performance, Wheel/Rail Forces, Truck Geometry, Transit Vehicle, Curving Performance, Flange Forces, Wheel/Rail Noise, Urban Rail Systems, Track, Railcar, Steady-State Curving Performance	18. Distribution Statement: **Available to the Public through the National Technical Information Service, Springfield, Virginia 22161.**

19. Security Classif. (of this report)	20. Security Classif. (of this page)	21. No. of Pages	22. Price
Unclassified	**Unclassified**	58	

Form DOT F 1700.7 (8-72) Reproduction of completed page authorized

PREFACE

Under the Urban Mass Transportation Administration (UMTA) Urban Rail Systems Program, Transportation Systems Center (TSC) is providing support to the Office of Technology Development and Deployment of the Urban Mass Transportation Administration. Under this program, TSC is responsible for the conduct of research, development and evaluation activities in support of the improvement of performance and reduction of cost of urban transit systems. The Wheel/Rail Dynamics Project being conducted as part of this program is directed toward the development of technical data that can be applied to improve performance specifications for transit car trucks and components to permit reductions in maintenance costs and wheel/rail noise while providing acceptable ride quality and safety. In order to define the potential improvement achievable in curving performance of transit trucks, a limiting value analysis is performed on current and candidate truck configurations to establish bounds on the expected curving performance. The results of this analysis are presented in this document.

METRIC CONVERSION FACTORS

Approximate Conversions to Metric Measures

Symbol	When You Know	Multiply by	To Find	Symbol
		LENGTH		
in	inches	2.5	centimeters	cm
ft	feet	30	centimeters	cm
yd	yards	0.9	meters	m
mi	miles	1.6	kilometers	km
		AREA		
in^2	square inches	6.5	square centimeters	cm^2
ft^2	square feet	0.09	square meters	m^2
yd^2	square yards	0.8	square meters	m^2
mi^2	square miles	2.6	square kilometers	km^2
	acres	0.4	hectares	ha
		MASS (weight)		
oz	ounces	28	grams	g
lb	pounds	0.45	kilograms	kg
	short tons (2000 lb)	0.9	tonnes	t
		VOLUME		
tsp	teaspoons	5	milliliters	ml
Tbsp	tablespoons	15	milliliters	ml
fl oz	fluid ounces	30	milliliters	ml
c	cups	0.24	liters	l
pt	pints	0.47	liters	l
qt	quarts	0.95	liters	l
gal	gallons	3.8	liters	l
ft^3	cubic feet	0.03	cubic meters	m^3
yd^3	cubic yards	0.76	cubic meters	m^3
		TEMPERATURE (exact)		
°F	Fahrenheit temperature	5/9 (after subtracting 32)	Celsius temperature	°C

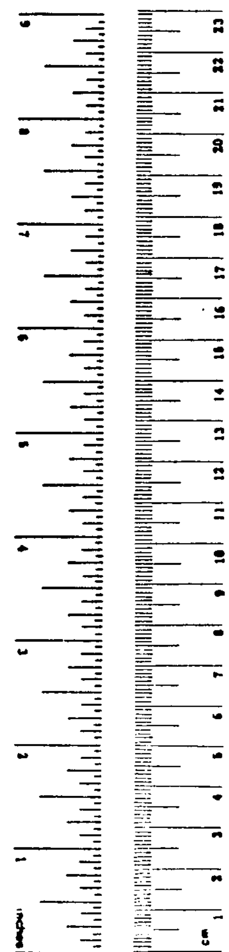

Approximate Conversions from Metric Measures

Symbol	When You Know	Multiply by	To Find	Symbol
		LENGTH		
mm	millimeters	0.04	inches	in
cm	centimeters	0.4	inches	in
m	meters	3.3	feet	ft
m	meters	1.1	yards	yd
km	kilometers	0.6	miles	mi
		AREA		
cm^2	square centimeters	0.16	square inches	in^2
m^2	square meters	1.2	square yards	yd^2
km^2	square kilometers	0.4	square miles	mi^2
ha	hectares (10,000 m^2)	2.5	acres	
		MASS (weight)		
g	grams	0.035	ounces	oz
kg	kilograms	2.2	pounds	lb
t	tonnes (1000 kg)	1.1	short tons	
		VOLUME		
ml	milliliters	0.03	fluid ounces	fl oz
l	liters	2.1	pints	pt
l	liters	1.06	quarts	qt
l	liters	0.26	gallons	gal
m^3	cubic meters	35	cubic feet	ft^3
m^3	cubic meters	1.3	cubic yards	yd^3
		TEMPERATURE (exact)		
°C	Celsius temperature	9/5 (then add 32)	Fahrenheit temperature	°F

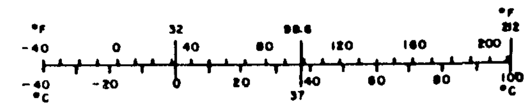

TABLE OF CONTENTS

LIST OF ILLUSTRATIONS

LIST OF TABLES

NOMENCLATURE

f = creep coefficient (linear theory)
F = lateral force
F_g = lateral flange force
h = ratio of wheel base to track gauge
K = stiffness of spring loaded stop for parallelogram truck
K_ψ = bending stiffness of radial truck
ℓ = half of track gauge
M = moment
N = normal force on wheel
P = net lateral (centrifugal) force
q = half of total flange clearance
r_o = nominal wheel radius of wheelset
R = curve radius
V = truck velocity
W = total load
y = lateral displacement of axle from track centerline
α = wheel conicity
β,γ = orientation of resultant creep force on leading and trailing wheels
μ = wheel/rail coefficient of friction
ψ = yaw angle of truck with normal to curve
ψ^* = deviation in yaw angle, from $h\ell/R$, of parallelogram truck
ϕ = warping angle of parallelogram truck

<u>Subscripts</u>

L = lateral
R = resultant
T = tangential
1,2 = leading and trailing axle, respectively.

SUMMARY

Under the UMTA Urban Rail Systems Program, TSC is conducting research and development activities for improving performance and reducing the cost of urban rail transit systems. The Wheel/Rail Dynamics Interaction Project being conducted as part of this program is directed toward reduction of maintenance costs and wheel rail noise while providing acceptable ride quality and safety. A significant part of this effort is directed toward determining design alternatives for providing improved curving performance of transit trucks. Some current designs have used a high interaxle stiffness to permit high speed performance without inducing hunting oscillations. In recent years, several truck designs have been advocated to improve steering capability during curve traversal by either providing direct interconnections between axles (radial trucks) or providing connections through linkages between the axles and carbody (guided steering). This document predicts bounds for the flange forces and wheel/rail forces of limiting case transit truck configurations to provide an estimate and comparison of the benefits in curving performance that can be achieved by modified truck configurations. These limiting configurations include:

1. Ideal rigid truck
2. Ideal parallelogramming truck
3. Ideal radial (self steering) truck
4. Ideal guided steering truck
5. Compensating guided steering truck

The ideal rigid truck is a model for some configurations used in passenger and transit applications. The two wheelsets are interconnected by a rigid primary system so that relative motion between the wheelsets cannot occur. The ideal parallelogramming truck is modeled with pinned connections between the interwheelset connections and the wheelset axles, which is a limiting case of zero shear stiffness. This configuration is statically stable on the track under the forces generated during curving until the flange clearance is taken up by both axles. In order to maintain static stability for sharper curves, spring loaded stops can be used. These stops are modeled as torsional springs rather than pins and allow a shearing (warping) action to occur between the axles. This parallelogramming action of the truck is typical of freight car trucks. Certain types of passenger car trucks, such as those with an equalizer bar assembly, also tend to behave in a parallelogram fashion. A self-steering truck is a truck with wheelsets that tend to align themselves with the instantaneous curve radius. These trucks use compliance between the axles to develop a yaw angle between the axles. This compliance typically involves a relatively low bending stiffness and relatively high shear stiffness. The ideal radial (self-steering) truck is the limiting case of zero bending stiffness and infinite shear stiffness. A guided steering truck uses linkages between the axles and the carbody to force a yaw angle between the axles for better alignment during curving. The ideal guided steering truck or "perfect" guided steering truck is a limiting case with rigid linkages and the axles aligned radially. A compensating guided steering truck uses rigid linkages to align the axles to obtain desired effects. By aligning the axles radially in the creep guidance region, and then in an oversteered configuration when the high rail is reached, this truck can traverse a curve of arbitrary radius without any flange force occurring.

For all cases in this document the wheel profiles are modeled by conical wheel treads with vertical wheel flanges. The track is smooth, free of all irregularity and provides single point contact to the wheel. For balance speed conditions three curving regions are investigated, creep guidance (no flanging), free curving (flanging on lead outer wheel), and constrained curving (flanging on both lead outer wheel and trailing inner wheel). The variation of wheel/rail force and flange force with curve radius is analyzed, including the effects of creep force saturation and gross sliding.

A comparison of the wheel/rail forces and the flange force for all five trucks in steady state curving is presented. The analysis is based on a conicity of 0.2 and a flange clearance of 0.405 inches. For the parameters used, the following relative comparisons can be made between the ideal trucks analyzed.

a) Only the two types of guided steering trucks analyzed are capable of steady state curving without any wheel/rail force (for the region: radius R greater than 435 feet).

b) In terms of limiting wheel/rail force on the high rail for R<435', the rigid, parallelogram and guided steering trucks produce about the same force levels (within 5% of 1.8 μN). The compensating guided steering truck and ideal radial truck have a limiting wheel/rail force on the high rail that is a factor of three less than the levels of the other trucks. For R>435', the parallelogram truck has a maximum wheel/rail force of 1.0 μN.

c) In terms of limiting flange force, the trucks produce about the same force level (Fg = 2.7 μN), except for the compensating guided steering truck and ideal radial truck which traverse the curve without flanging by adopting an oversteered position of the axles. For R>435', the parallelogram truck has a maximum flange force of 2.0 μN.

d) In terms of the track curvature that the trucks can traverse without force saturation occurring, the trucks can be ranked from lowest to highest curvature as parallelogram, rigid, guided steering, compensating guided steering and radial. The parallelogram truck reaches a radius of about 1000 feet when saturation occurs, whereas the compensating guided steering truck and ideal radial truck can traverse a curve with a radius as low as 217 feet before force saturation occurs.

1. INTRODUCTION

Current truck designs for transit applications have concentrated on ease of assembly, minimization of moving parts and use of relatively rigid structural members in an effort to ensure reliability and maintainability. Some designs have used a high interaxle stiffness to permit high speed performance without inducing hunting oscillations. In recent years, several truck designs have been advocated to improve steering capability during curve traversal by either providing direct interconnections between axles (radial trucks) or providing connections through linkages between the axles and carbody (guided steering).

In order to optimize curving performance, truck designers must consider the effects of many interacting parameters. Among truck parameters are wheel taper, inter-axle distance and stiffness, angle of attack in curving, flange clearance and frictional elements. Rail and track parameters include rail wear, curve radius and environmental conditions. The wheel/rail interaction forces and slip/force saturation behavior link the truck and rail parameters, and are important factors in establishing overall performance. Analytical studies which include many of these parameters and also present the results of the mechanics of curve negotiation in a closed form relationship provide a useful service. Design choices involving preliminary trade-offs and parameter optimization for minimization of curving forces can then be made quickly without the need for detailed, and possibly costly, computer codes.

This document predicts the upper bounds of the flange forces and wheel/rail forces of limiting case transit truck configurations in a closed form relationshop to provide an estimate of the benefits in curving performance that can be achieved by modified truck configurations. These limiting configurations include:

1. Ideal rigid truck
2. Ideal parallelogramming truck
3. Ideal radial (self steering) truck
4. Ideal guided steering truck
5. Compensating guided steering truck.

In all cases the wheel profiles are modeled by conical wheel treads with vertical wheel flanges. The rail is modeled as perfectly smooth, free of all irregularity and provides single point contact to the wheel. For balance speed conditions three curving regions are investigated, creep guidance (no flanging), free curving (flanging on lead outer wheel), and constrained curving (flanging on both lead outer wheel and trailing inner wheel). The variation of wheel/rail force and flange force with curve radius is analyzed, including the effect of creep force saturation and gross sliding.

2. RIGID TRUCK

The rigid truck shown in Figure 1 is typical of configurations used in passenger and transit applications. The two wheelsets are interconnected by a rigid primary system so that relative motion between the wheelsets cannot occur. The governing equations for analyzing any truck in steady state curving are based on a balance of forces and moments. The total lateral truck force, including any net external force P, is zero. For negligible centerplate friction (a good approximation for most modern transit trucks), the total moment on the truck is zero. The rigid truck is analyzed in Reference [1], and the solutions of the truck equilibrium equations for the flange forces are (assuming $f_L = f_T$):

$$F_{g_1} = \frac{2f}{h}\left[\frac{(1+h^2)\ell}{R} - \frac{\alpha y}{r_o}\right] + 2f\psi + \frac{P}{2} \tag{1}$$

$$F_{g_2} = \frac{2f}{h}\left[\frac{(1+h^2)\ell}{R} - \frac{\alpha y}{r_o}\right] - 2f\psi - \frac{P}{2}. \tag{2}$$

For the creep guidance range (no flange contact) the wheel/rail forces are $fh\ell/R-P/4$ for the wheels of the lead axle and $-\ fh\ell/R-P/4$ for the wheels of the trailing axle. The free curving region (flanging on lead outer wheel only), defined by

$$y_1 = q,\ y = q - h\ell\psi,\ F_{g_2} = 0, \tag{3}$$

occurs for

$$R < \frac{(1+h^2)r_o}{\alpha\left(\frac{q}{\ell} + \frac{Ph}{4f}\right)}, \tag{4}$$

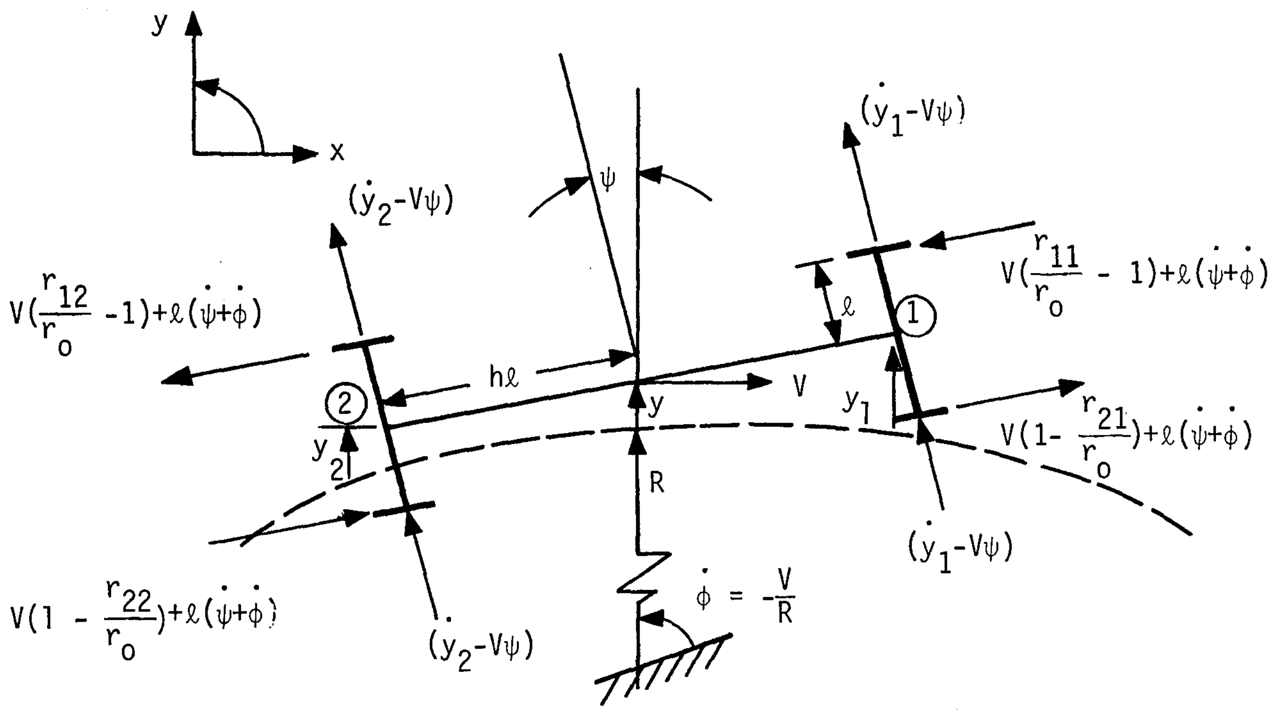

(1a) Creep Velocity

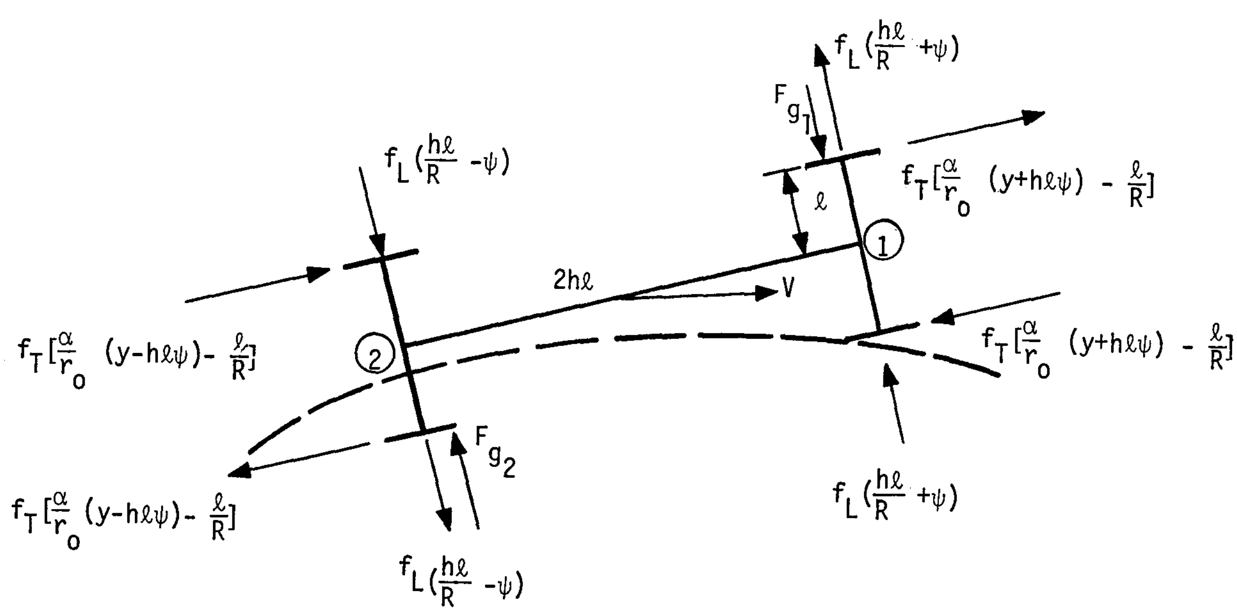

(1b) Creep Forces

FIGURE 1. RIGID TRUCK IN STEADY-STATE CURVING

and the lead axle wheel/rail forces are

$$\text{leading axle outboard} = -F_{g_1} + f\left(\frac{h\ell}{R} + \psi\right)$$

$$= -\frac{3}{4}F_{g_1} + \frac{fh\ell}{R} - \frac{P}{4}, \tag{5}$$

$$\text{leading axle inboard} = f\left(\frac{h\ell}{R} + \psi\right)$$

$$= -\frac{1}{4}F_g + \frac{fh\ell}{R} - \frac{P}{4},$$

with the flange force

$$F_{g_1} = 4f\psi + P$$

$$= 4f\left[\frac{(1+h^2)\ \frac{\ell}{R} - \frac{\alpha q}{r_o}}{h\left(1 - \frac{\alpha\ell}{r_o}\right)}\right] - \frac{P(\alpha\ell/r_o)}{1 - \alpha\ell/r_o}\ . \tag{6}$$

For the <u>constrained</u> region, characterized by flanging on the lead outer wheel and trailing inner wheel, the yaw angle ψ reaches its maximum value ψ_{max} which is fixed by the track geometry,

$$\psi = \psi_{max}$$

$$= q/h\ell, \tag{7}$$

and the force levels may be found in the same manner as in equations (1) - (2). Using (7) the constrained region for the rigid truck occurs for

$$R < \frac{(1+h^2)\ell}{\left(\frac{q}{\ell} + \frac{Ph}{4f}\right)}. \tag{8}$$

The previous results hold only for the case of no wheel slipping (sliding). However, the maximum value that the resultant force can acquire before saturation occurs in μN where μ is the friction coefficient and N is the wheel load. It is assumed that once a wheel slips, the resultant force is aligned with the resultant creep velocity. Typically the lead axle will slip in the free curving region. As the constrained curving region is approached, force saturation occurs on <u>both</u> the leading and trailing wheels and the lead axle forces then tend to be independent of curve radius. In this report, the investigation of the limiting force levels on the wheels of the lead axle is done with the assumption of slipping of both the front and back wheels in the free curving region at balance speed conditions P=0.

Sliding forces for the rigid truck are shown in Figure (2) with the orientation of the forces defined by the orientation of the equivalent creep forces. Solving (1) for this rigid truck sliding condition in the free curving region* leads to

$$F_{g_1} = 2\mu N \sin\beta + 2\mu N \sin\gamma, \tag{9a}$$

$$2\mu N \sin\gamma = \frac{\mu N}{h} (\cos\beta + \cos\gamma) . \tag{9b}$$

The yaw angle ψ is determined from an iterative solution of the transcendental equation (9b), where the orientation angles at the leading and trailing axles, β and γ, respectively are defined as

$$\beta = \tan^{-1} \frac{(h\ell/R) + \psi}{\ell/R - \alpha q/r_o} \tag{10}$$

$$\gamma = \tan^{-1} \frac{(h\ell/R) - \psi}{\ell/R - \frac{\alpha}{r_o} (q-2h\ell\psi)} .$$

*An alternative derivation based on sliding forces in the constrained region is presented in Appendix A.

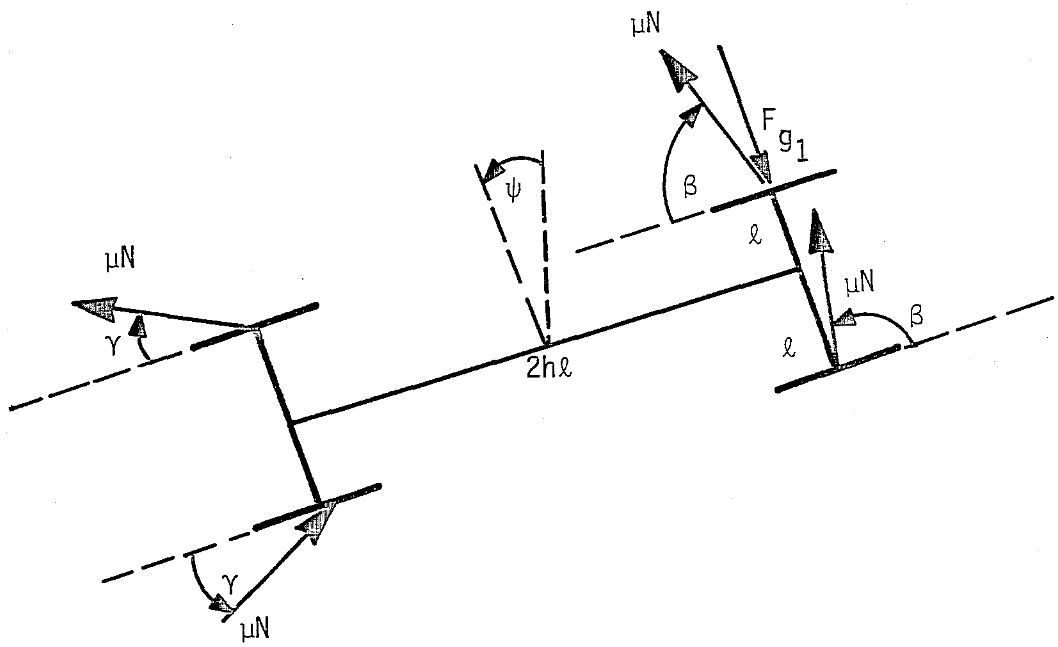

$$\tan\beta = \frac{\frac{h\ell}{R} + \psi}{\frac{\ell}{R} - \frac{\alpha}{r_o}\,q}\,, \qquad \tan\gamma = \frac{\frac{h\ell}{R} - \psi}{\frac{\ell}{R} - \frac{\alpha}{r_o}\,(q-2h\ell\psi)}$$

FIGURE 2. SLIDING FORCES ON RIGID TRUCK

The calculation of the flange force F_{g_1} then follows from (9a). Following Figure 2, the lateral wheel/rail forces are,

$$\begin{aligned} &\text{Lateral W/R Force (Lead Outboard Wheel)} = F_{g_1} - \mu N \sin\beta \\ &\text{Lateral W/R Force (Lead Inboard Wheel)} = \mu N \sin\beta . \end{aligned} \qquad (11)$$

3. PARALLELOGRAM TRUCK

The ideal parallelogram truck is modeled with pinned connections between the axles leading to a limiting case of zero shear stiffness (Figure 3). The parallelogramming action of a truck is typical of freight car trucks. Certain types of passenger car trucks, such as those with equalizer bar assembly, also tend to behave in a parallelogram fashion. The pinned configuration is stable on the track under the forces generated during curving until the flange clearance is taken up by both axles ($R \geq r_0 \ell/\alpha q$). In order to maintain static stability in the free curving region for still sharper curves, spring loaded stops can be used. These stops are modeled as torsional springs (Figure (5)) rather than pin connections and allow a shearing (warping) action, defined by the angle ϕ, to occur between the two axles.

As shown in Figure 3, the lead and trailing axles are subject to the (same) yaw angle ψ and, in addition, the entire truck can warp through the angle ϕ. Applying equilibrium relations balancing forces and moments and assuming negligible centerplate friction yields

$$F_{g_1} = 2f \left(\frac{h\ell}{R} + \psi\right) + P/2\,, \tag{12a}$$

$$F_{g_2} = 2f \left(\frac{h\ell}{R} - \psi\right) - P/2\,, \tag{12b}$$

$$\left(F_{g_2} + F_{g_1}\right) = \frac{4f\ell}{hR} \left(1+h^2\right) - \frac{2f\alpha}{hr_0} (y_1+y_2). \tag{13}$$

It follows from (12a) and (12b) that the <u>creep guidance</u> case of steady state curving without flange contact is not possible,* i.e., flanging always occurs.

*For $F_{g_1} = 0$, $\psi = -h\ell/R$ and for $F_{g_2} = 0$, $\psi = + h\ell/R$.

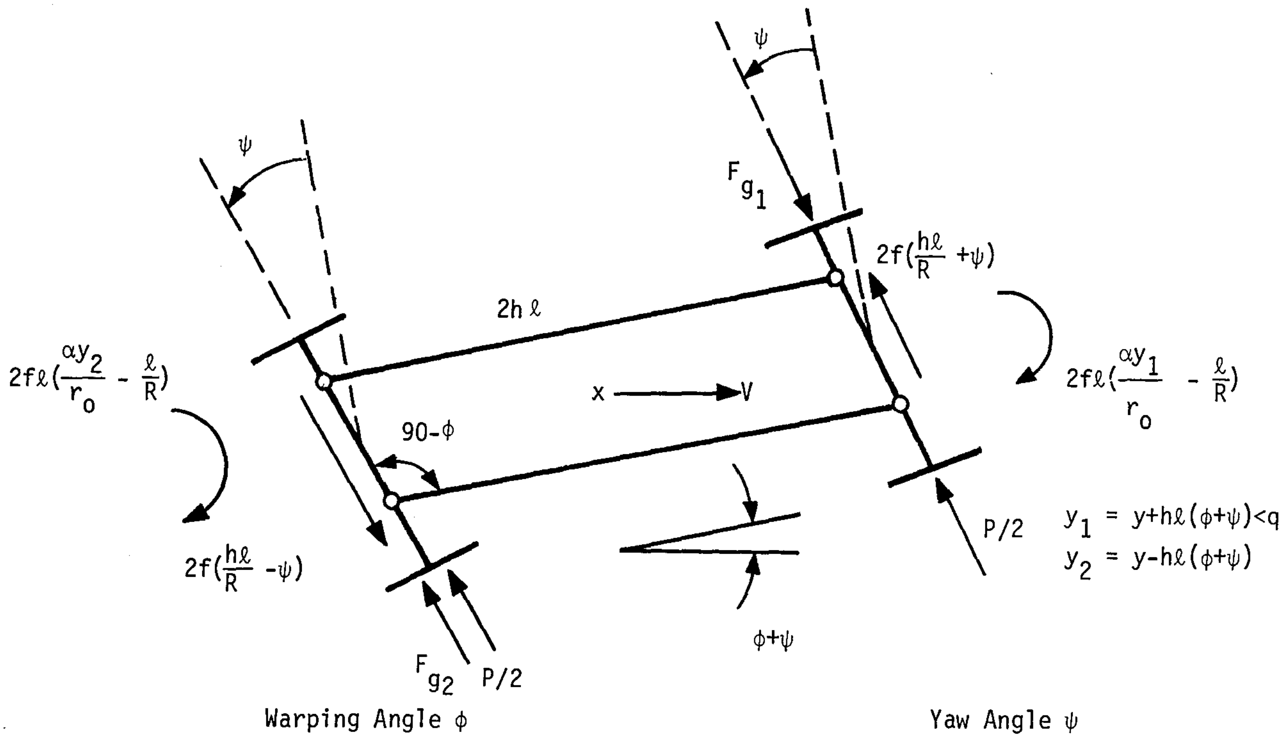

(3a) Creep Forces

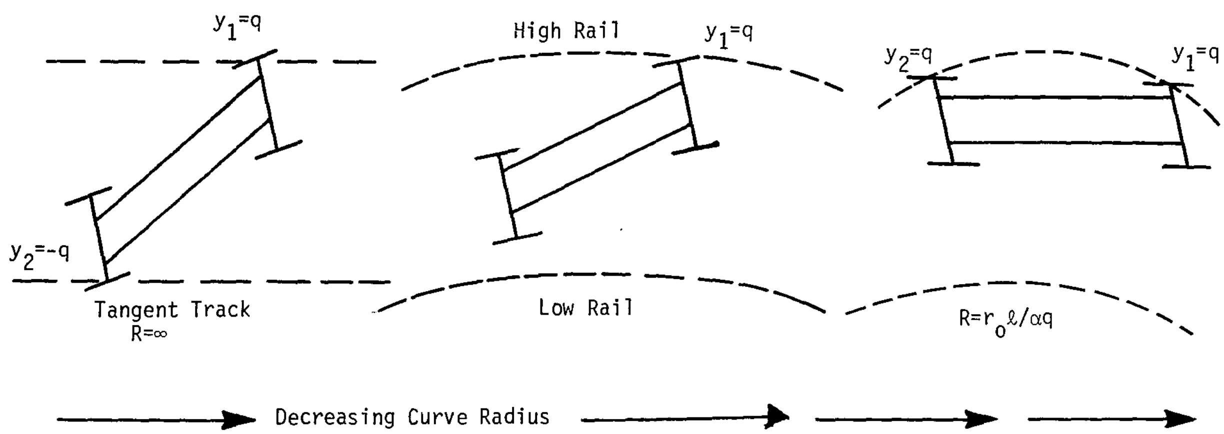

(3b) Effect of Curve Radius on Position of Truck

FIGURE 3. PARALLELOGRAM TRUCK WITH PINNED CONNECTIONS

In the free curving regime, defined by

$$y_1 = q, \; F_{g_2} = 0, \tag{14}$$

solution of (12) yields

$$y_2 = -q + \frac{2r_o \ell}{\alpha R}. \tag{15}$$

This relationship shows that as the track radius decreases, the rear axle moves towards the high rail, as shown in Figure (3b). When $y_2=q$, the flange clearance available for the trailing axle is completely taken up and the radius becomes, $R_c=r_o\ell/\alpha q$. An equilibrium solution for the free curving case is possible only if $R>r_o\ell/\alpha q$ with

$$\psi = \frac{h\ell}{R} - \frac{P}{4f} \quad , \quad F_{g_1} = 4f\,\frac{h\ell}{R}. \tag{16}$$

The lead axle wheel/rail forces are

$$\text{leading axle outboard} = -F_{g_1} + f\left(\frac{h\ell}{R} + \psi\right) \tag{17}$$

$$= -2f\,\frac{h\ell}{R} - \frac{P}{4},$$

$$\text{leading axle inboard} = f\left(\frac{h\ell}{R} + \psi\right) \tag{18}$$

$$= 2f\,\frac{h\ell}{R} - \frac{P}{4}.$$

If force saturation occurs within this range of $R>R_c$, then the limiting force levels for the parallelogram truck are determined from an analysis of the case when slipping occurs on wheels of the leading axle. These sliding forces are shown in Figure (4) with the orientation defined by the creep forces. In order for the trailing wheelset to balance in equilibrium (without flanging)

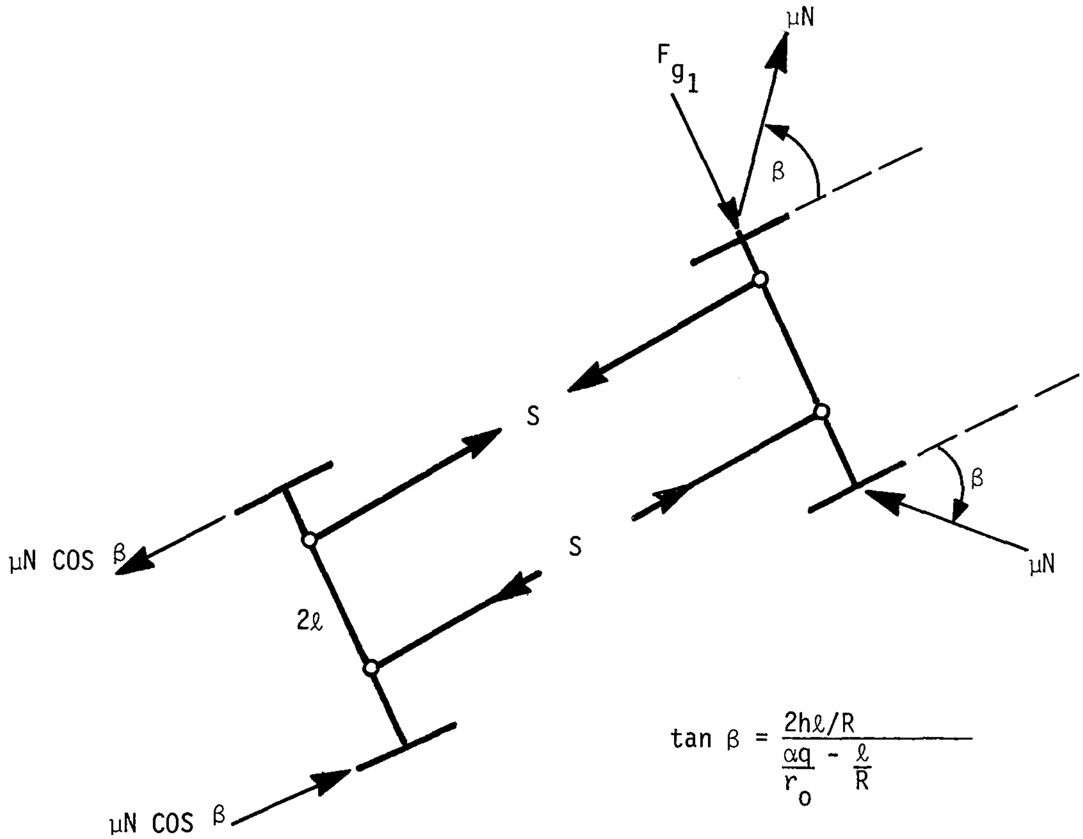

FIGURE 4. SLIDING FORCES ON PINNED PARALLELOGRAM TRUCK

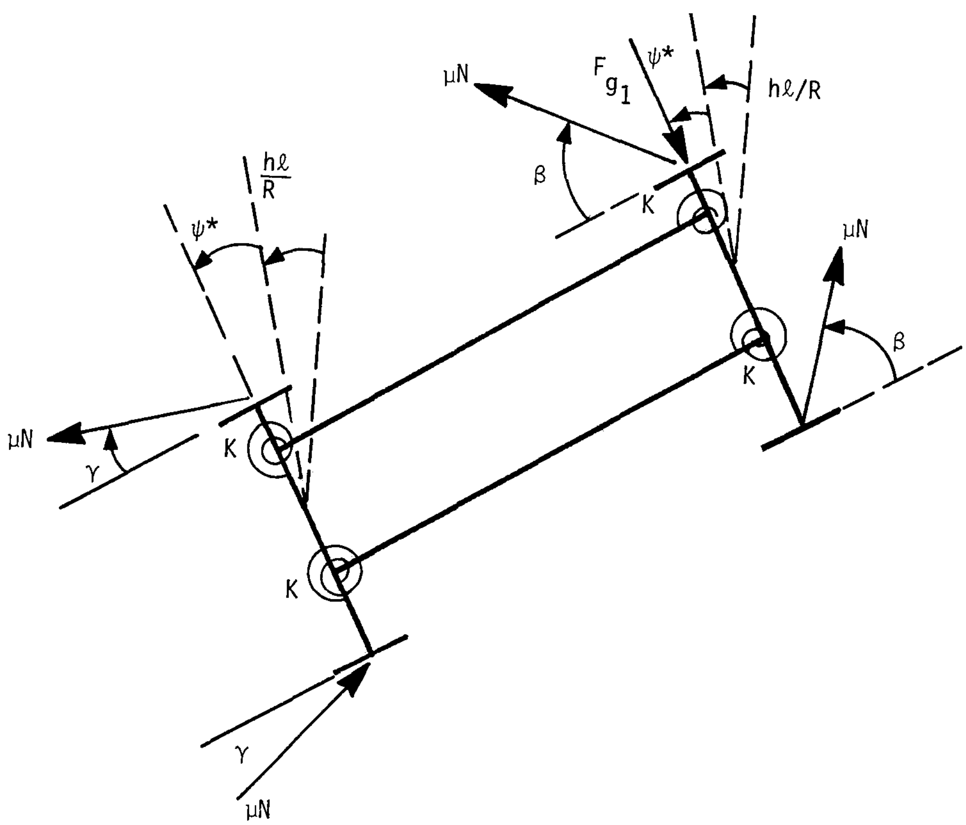

FIGURE 5. SLIDING FORCES ON PARALLELOGRAM TRUCK
WITH SPRING-LOADED STOPS

the wheel/rail forces must be purely longitudinal and the trailing wheelset adopts the radial position

$$\psi = \frac{h\ell}{R}. \tag{19}$$

The sliding forces on the leading axle are oriented at the angle β, where

$$\beta = \tan^{-1} \frac{2h\ell/R}{\frac{\ell}{R} - \frac{\alpha q}{r_o}}. \tag{20}$$

The lateral wheel/rail forces on the leading axle are

$$\begin{aligned} &\text{Lateral W/R Force (Lead Outboard Wheel)} = F_{g_1} - \mu N\sin\beta \\ &\text{Lateral W/R Force (Lead Inboard Wheel)} = \mu N\sin\beta. \end{aligned} \tag{21}$$

The maximum value that the flange force can attain occurs when the lead saturation force is aligned laterally, i.e., $\beta = 90°$. This occurs when $R = r_o\ell/\alpha q$ (equation (20)) and produces a lead axle flange force $F_{g_1} = 2\mu N$.

For $R<R_c$, equilibrium cannot be maintained in the free curving regime unless spring loaded stops are used to prevent collapse of the truck. These can be modeled as torsional springs as shown in Figure (5) and permit a finite shearing (warping) action to occur between the axles as defined by the angle ϕ. In order to ensure the stability of the truck in a free curving equilibrium condition, the springs must have a minimum value of stiffness K. Appendix B, shows that

$$K \geq h\ell f \tag{22}$$

is a minimum requirement for obtaining a stable equilibrium condition to prevent collapse of the parallelogram truck.

If force saturation occurs on the parallelogram truck with spring loaded stops within the region $R<R_c$, a limiting value of the flange force and wheel/rail force is obtained from an analysis involving saturation on both the lead and trailing axles. Sliding forces (Figure 5) are oriented by the equivalent creep forces in a similar manner to that for the rigid truck. Sliding in the free curving region under balance speed conditions (P=0) leads to the identical equations as for the rigid truck, (9a) and (9b) where now the angles β and γ are defined as

$$\tan\beta = \frac{\psi^{*}+2h\ell/R}{\frac{\ell}{R} - \frac{\alpha q}{r_o}} \quad , \quad \tan\gamma = \frac{\psi^{*}}{\frac{\ell}{R} - \frac{\alpha}{r_o}\;(q-2h\ell(\phi+\psi^{*}))} . \qquad (23)$$

In this expression, ψ^{*} is defined as the deviation of the axle from the yaw position defined in equation (19). For a given value of shear angle ϕ the yaw angle ψ^{*} for this warped truck is determined from an iterative solution of the transcendental equation (9b). The calculation of the flange force F_{g_1} then follows from (9a). The lateral wheel/rail forces on the lead axle are given by the expressions in (21).

4. IDEAL RADIAL (SELF-STEERING) TRUCK

A self steering truck has wheelsets that tend to align themselves with the instantaneous curve radius. These trucks use compliance between the axles to develop a yaw angle between the axles, as shown in Figure 6. This compliance typically involves a relatively low bending stiffness and relatively high shear stiffness. The ideal radial (self steering) truck, is the limiting case of infinite shear stiffness ($K_y \sim \infty$) with zero bending stiffness, K_ψ.

A complete solution is obtained by applying the equilibrium relations to the leading and trailing segments of the truck (parts I and II, respectively, on Figure (7a)). In this derivation a finite bending stiffness K_ψ is included, and the ideal radial truck is obtained in the limit as $K_\psi \to 0$. The equilibrium relations are

$$F_{g_1} = \frac{2f}{h}\left[\frac{\ell}{R} - \frac{\alpha y_1}{r_o}\right] + 2f\psi_1 + \frac{P}{2} - \frac{K_\psi}{h\ell}(\psi_1 - \psi_2) + \frac{2K_\psi}{R},$$

$$F_{g_2} = \frac{2f}{h}\left[\frac{\ell}{R} - \frac{\alpha y_2}{r_o}\right] - 2f\psi_2 - \frac{P}{2} + \frac{K_\psi}{h\ell}(\psi_1 - \psi_2) - \frac{2K_\psi}{R}, \qquad (24a)$$

$$y_1 = y - h\ell\left(\frac{h\ell}{R} - \psi_1\right), \quad y_2 = y - h\ell\left(\frac{h\ell}{R} + \psi_2\right), \qquad (24b)$$

where ψ_1 and ψ_2 are yaw angles defined in terms of deviations from the pure radial position. Overall equilibrium is maintained by the relationship

$$F_{g_2} - F_{g_1} = -2f\left(\psi_1 + \psi_2\right) - P, \qquad (25)$$

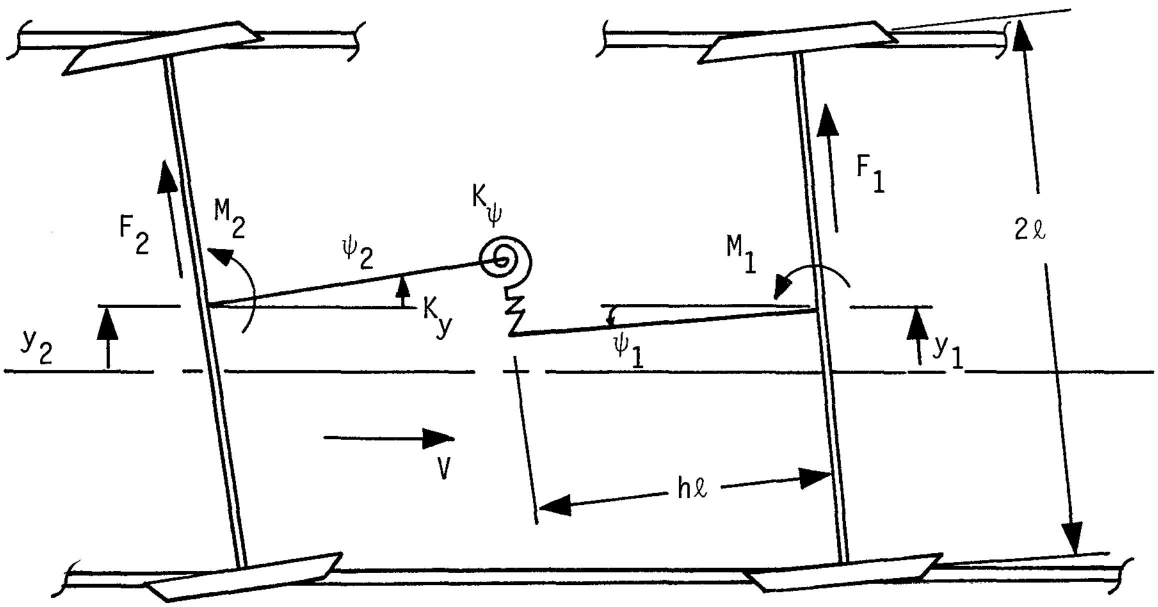

K_y = Shear Stiffness, K_ψ= Bending Stiffness

FIGURE 6. FLEXIBLE TWO-AXLE TRUCK ASSEMBLY

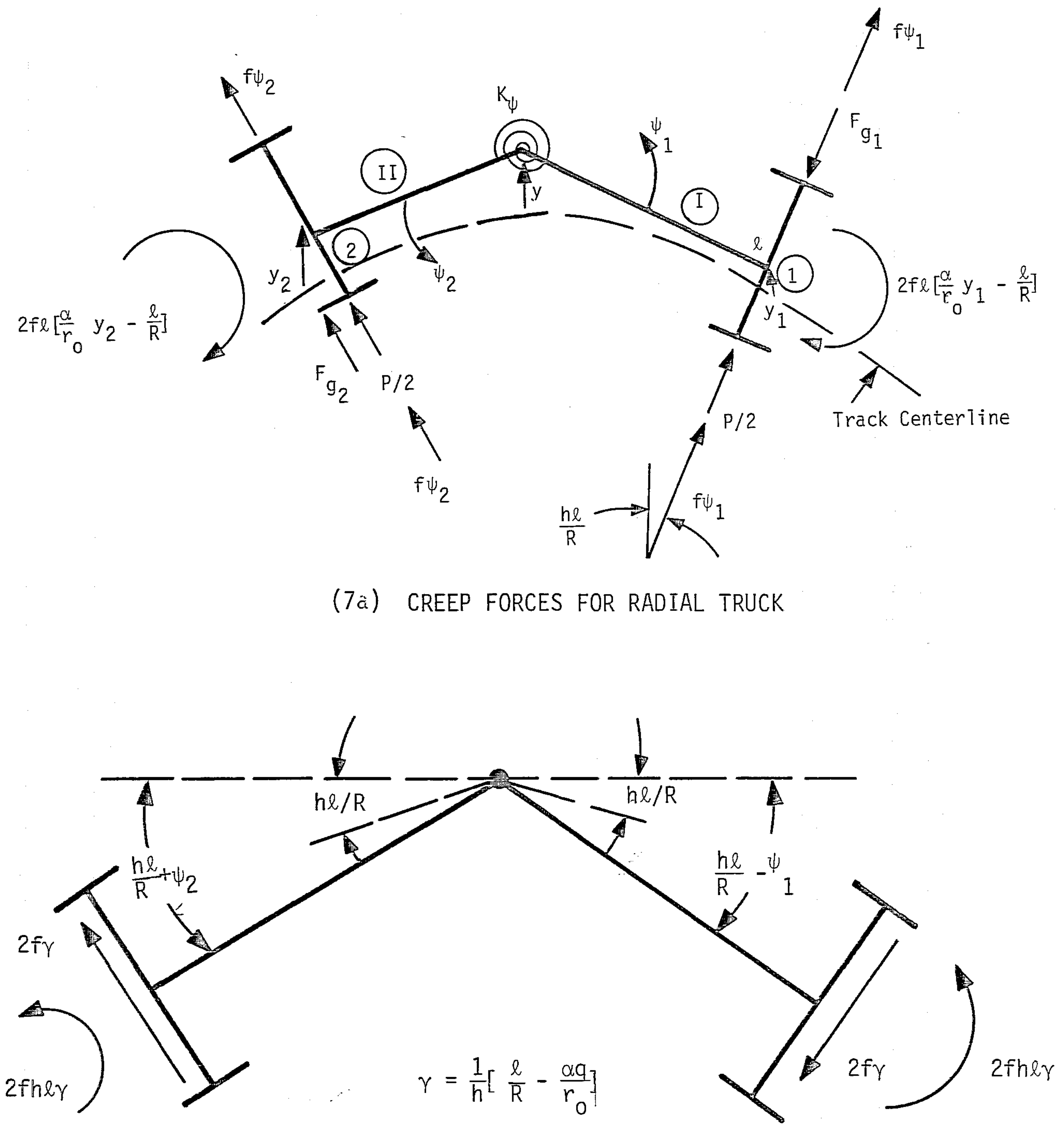

(7a) CREEP FORCES FOR RADIAL TRUCK

(7b) FREE BODY DIAGRAM IN FREE CURVING REGION FOR IDEAL RADIAL TRUCK ($K_\psi \to 0$)

FIGURE 7. RADIAL (SELF-STEERING) TRUCK (ψ_1 AND ψ_2 MEASURED FROM RADIAL POSITION)

as long as sliding does not take place.

The creep guidance case for the ideal radial truck is obtained from these equations with $F_{g_1} = 0$, $F_{g_2} = 0$ and $K_\psi = 0$. Solution of equation (24) and (25) leads to

$$y_1 = y_2, \tag{26}$$

which implies that the truck has no preferred lateral position. A more refined analysis shows that equation (26) represents an equilibrium state that is not unique. For any non-zero bending stiffness $K_\psi > 0$, a unique solution can be found, in the form

$$\begin{aligned} y_1 &= \left(1 + h^2\right) \frac{r_o \ell}{\alpha R}, \quad y_2 = y_1 \\ \psi_1 &= h\ell/R, \quad \psi_2 = - h\ell/R. \end{aligned} \tag{27}$$

For this creep guidance range, the radial truck traverses the curve with the same lateral excursion as the rigid truck, Ref. [1], and the bending spring K_ψ remains undeformed.

The free curving region defined by (14) occurs for

$$R \leq \frac{\left(1 + h^2\right) r_o}{\frac{\alpha q}{\ell} + \frac{P\alpha h}{4f}\left(1 - \frac{h\ell f}{K_\psi}\right)}. \tag{28}$$

Solving the equations of motion with finite bending stiffness in the free curving region, in which the lead wheelset flanges against the high rail, produces

$$F_{g_1} = 4f\left[\frac{(1 + h^2)\,\frac{\ell}{R} - \frac{\alpha q}{r_o}}{h\left(1 - \frac{\alpha\ell}{r_o}\right) + \frac{\alpha h^2 \ell^2 f}{K_\psi r_o}}\right] - \frac{P\left(\frac{\alpha\ell}{r_o}\right)\left(1 - \frac{h\ell f}{K_\psi}\right)}{\left(1 - \frac{\alpha\ell}{r_o}\right) + \frac{\alpha h \ell^2 f}{K_\psi r_o}}, \tag{29}$$

Both the expression for the free curving region and the lead axle flange force, reduce to the respective rigid truck results [(4), (6)] when $K_\psi \sim \infty$. Further results related to the curving performance of the radial truck with finite bending stiffness may be deduced from Reference [2]. Solution of the equilibrium equations also yields information on yaw angles and displacement, as follows

$$\psi_1 = \frac{1}{h}\left(\frac{\alpha q}{r_o} - \frac{\ell}{R}\right) + \frac{F_{g_1}}{4f}\left(2 - \frac{\alpha\ell}{r_o}\right) - \frac{P}{4f}\left(1 - \frac{\alpha\ell}{r_o}\right)$$

$$\psi_2 = - \psi_1 + \frac{1}{2f}\left(F_{g_1} - P\right) \tag{30}$$

$$y_2 = q - \frac{h\ell}{2f}\left(F_{g_1} - P\right).$$

Based on the relations in (27) and (30) the behavior of the radial truck with finite bending stiffness can be ascertained as a function of curve radius, R. For the creep guidance range with balance speed condition, P = 0, both wheelsets have the same lateral displacement. Decreasing the curve radius R, leads to an increase in lateral displacement. When the high rail is finally met, i.e., flange clearance is taken up, the lead axle flanges and the trailing axle moves away from the high rail towards the low rail. The wheel/rail forces build up with decreasing radius and typically force saturation occurs somewhere between the radius defined for free curving and that for constrained curving.

The behavior of the <u>ideal radial truck</u> ($K_\psi \rightarrow 0$) with decreasing curve radius is quite different from the behavior for finite K_ψ. When the truck reaches the high rail a flange force is not built up (i.e., $F_{g_1} \sim 0$, $K_\psi \to 0$) for balance speed conditions. For smaller curve radius the truck moves along the high rail and offsets the increasing track curvature by orienting the axles to an oversteered position. The positions of the axles are defined in (30) by

$$\psi_1 = \frac{1}{h}\left(\frac{\alpha q}{r_o} - \frac{\ell}{R}\right) \qquad \psi_2 = -\psi_1, \tag{31}$$

for the balance speed curving where the yaw angles ψ_1 and ψ_2' are defined from the radial position. The axles adopt an over-steered orientation for

$$R < r_o\ell/\alpha q. \tag{32}$$

A typical force diagram for this orientation is shown in Figure (7b). For curving with lateral imbalance loads ($P > 0$), the net load P is shared equally by both wheelsets by flange forces at both wheelsets on the high rail.

The wheel/rail forces on the ideal truck build up as the radius of the curve decreases. The resultant saturation force is oriented in the direction of the resultant creep force. Based on the orientation shown in Figure 7b, the sliding forces on each axle are oriented at the angle β, where

$$\beta = \tan^{-1} 1/h \tag{33}$$

The lateral wheel/rail force on the wheels of the leading and trailing axles is

$$\text{Lateral W/R Force} = \mu N \text{Sin}\beta \tag{34}$$

The maximum value of lateral W/R force is $0.58\mu N$.

5. IDEAL GUIDED-STEERING TRUCK

A guided steering truck uses linkages between the axles and the carbody to force an angle between the axles for better alignment during curving. The ideal guided steering truck or "perfect" guided steering truck is a limiting case with rigid linkages and the axles aligned radially, as shown in Figure 8. (The terms "oversteered" and "understeered" refer to cases where the angle between the interwheelset connection and the axle is greater than, or less than, respectively, the radial alignment angle $h\ell/R$.)

Applying equilibrium relations balancing forces and moments leads to

$$F_{g_1} = \frac{2f}{h}\left[\frac{\ell}{R} - \frac{\alpha}{r_o}\, y\right] + 2f\psi + \frac{P}{2}\,, \tag{35}$$

$$F_{g_2} = \frac{2f}{h}\left[\frac{\ell}{R} - \frac{\alpha}{r_o}\, y\right] - 2f\psi - \frac{P}{2}\,, \tag{36}$$

which is identical to the flange force relations for the rigid truck (equations (1), (2)) except for the $(1+h^2)$ factor multiplying ℓ. In the creep guidance range, the lead and trailing axles are aligned perfectly with radial lines from the center of curvature of the curved track. For balance speed conditions (P=0) the truck moves along the rolling line offset position for pure rolling with zero yaw angle,

$$y = \frac{r_o \ell}{\alpha R}\ , \quad \psi = 0\ . \tag{37}$$

The creep forces are zero and the axles are aligned radially.

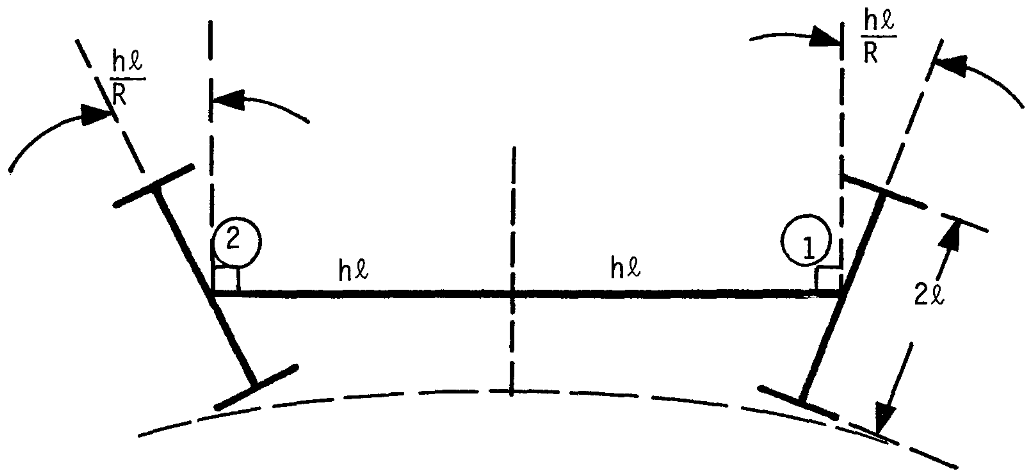

(8a) Original Geometry of Truck

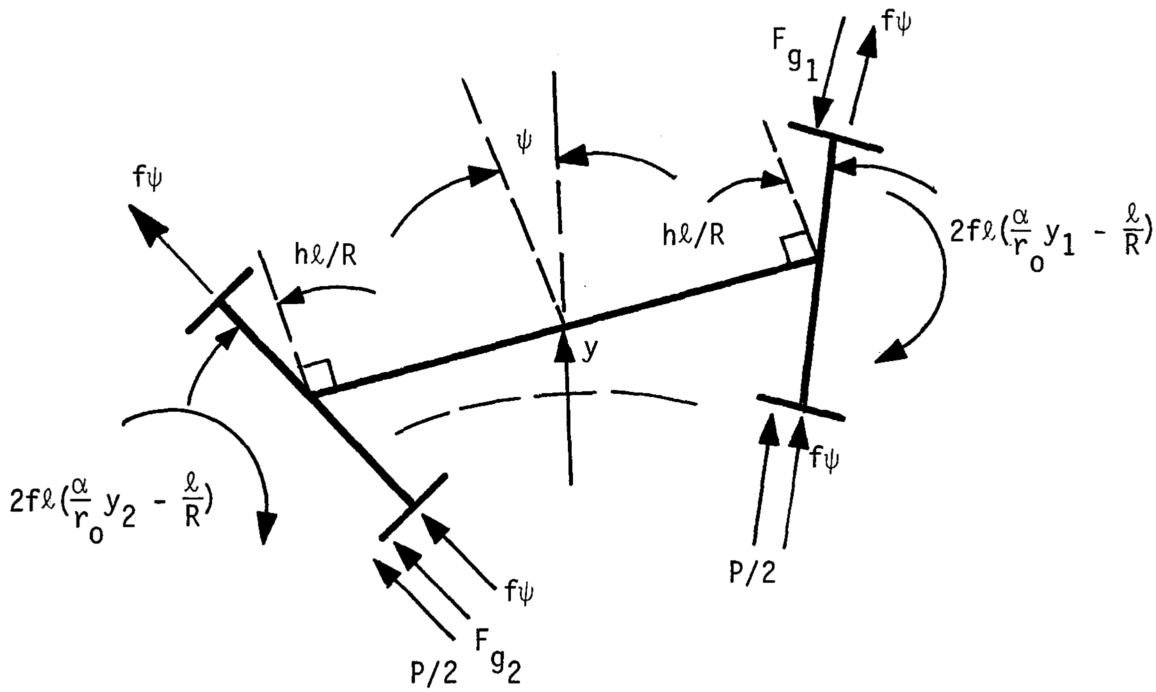

$y_1 = y + h\ell\psi$, $y_2 = y - h\ell\psi$

(8b) Truck in Yawed Position with Forces Acting

FIGURE 8. IDEAL GUIDED-STEERING TRUCK

The free curving region defined by (3) occurs for

$$R < \frac{r_o}{\alpha\left(\frac{q}{\ell} + \frac{Ph}{4f}\right)} , \tag{38}$$

which is a factor of $(1+h^2)$ less than the radius required for a rigid truck (equation (4)). Solving equations (35), (36) the lead axle wheel/rail forces are (Figure 8).

$$\text{Lead W/R Force Outboard} = - F_{g_1} + f\psi$$

$$= - 3/4\ F_g - \frac{P}{4} , \tag{39}$$

$$\text{Lead W/R Force Inboard} = f\psi$$

$$= 1/4\ F_g - \frac{P}{4} , \tag{40}$$

with the flange force

$$F_{g_1} = 4f\psi + P$$

$$= 4f \left[\frac{\frac{\ell}{R} - \frac{\alpha q}{r_o}}{h\left(1-\alpha\ell/r_o\right)} \right] - \frac{P\left(\alpha\ell/r_o\right)}{\left(1 - \alpha\ell/r_o\right)} . \tag{41}$$

The constrained region for the guided steering truck defined by (7) occurs for

$$R < \frac{\ell}{\left(\frac{q}{\ell} + \frac{Ph}{4f}\right)} , \tag{42}$$

and flange contact occurs on both the leading and trailing axle.

For the truck with ideal guided steering and rigid linkages, flanging on the lead axle and also sliding on both the leading and trailing axle, equations defining the balance of forces and moments are the same form as for the rigid truck (9a) and (9b). The angles β and γ are now defined by

$$\tan\beta = \frac{\psi}{\left(\frac{\ell}{R} - \frac{\alpha}{r_o} q\right)}, \quad \tan\gamma = \frac{\psi}{\left(\frac{\ell}{R} - \frac{\alpha}{r_o}\left\{q - 2h\ell\psi\right\}\right)}. \tag{43}$$

The yaw angle ψ is determined from the transcendental equation (9b) and the calculation of the flange force F_{g_1} follows from (9a). From Figure 8, the lateral wheel/rail forces are

$$\text{Lateral W/R Force, Lead Outboard Wheel} = F_{g_1} - \mu N \sin\beta$$

$$\text{Lateral W/R Force, Lead Inboard Wheel} = \mu N \sin\beta. \tag{44}$$

6. COMPENSATING GUIDED-STEERING TRUCK

A compensating guided steering truck (Figure 9) uses linkages between the axles and the carbody to set an appropriate angle between the interwheelset connecting bar and the axle to obtain desired results. For example, by properly oversteering this type of guided steering truck, steady state curving can be maintained without flange force.

The analysis is carried out in a similar manner to the analysis in Section 5 for the ideal guided steering truck. Due to the importance of the creep coefficients in fixing the correct amount of oversteering, the analysis is done with the lateral creep coefficient f_L distinct from the tangential creep coefficient f_T. Applying a balance of forces and moments to the truck free body diagram shown in Figure (9), where the angles ϕ_1 and ϕ_2 are measures of the deviation of the axles from the radial position, leads to

$$\begin{aligned} F_{g_1} &= \frac{2f_T}{h}\left[\frac{\ell}{R} - \frac{\alpha}{r_o}\, y\right] + 2f_L(\psi - \phi_1) + P/2, \\ F_{g_2} &= \frac{2f_T}{h}\left[\frac{\ell}{R} - \frac{\alpha}{r_o}\, y\right] - 2f_L(\psi + \phi_2) - P/2, \end{aligned} \tag{45}$$

In the creep guidance region, the solution of (45) leads to

$$y = \frac{r_o \ell}{\alpha R} - \frac{f_L}{2f_T}\left(r_o \frac{h}{\alpha}\right)\left(\phi_1 + \phi_2\right), \quad \psi = -\frac{P}{4f_L}. \tag{46}$$

For balance speed conditions with the axles aligned radially, the truck moves along the rolling line offset position for pure rolling with zero yaw angle

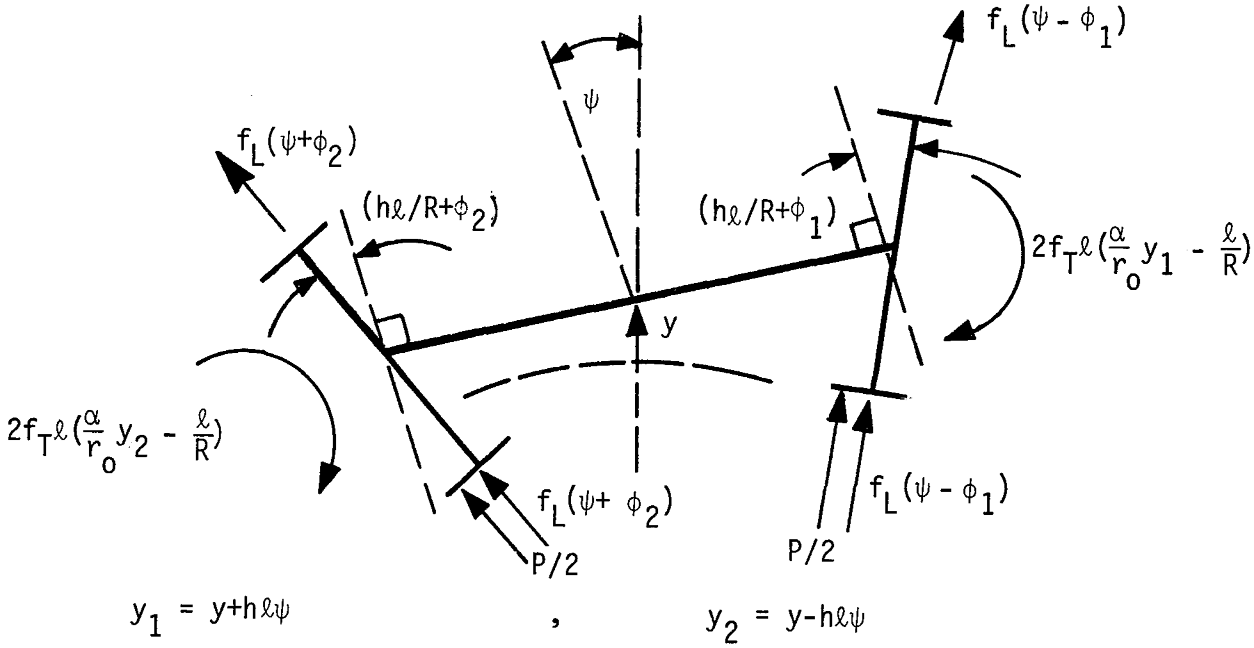

(9a) Free Body Diagram of Compensating Guided Steering Truck

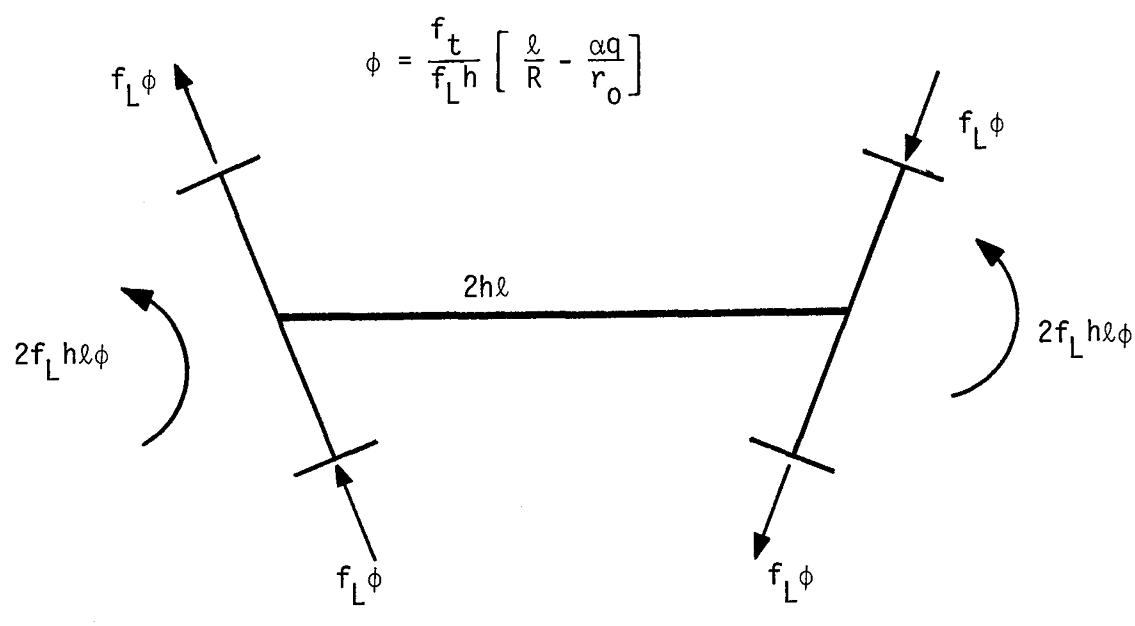

(9b) Truck in Steady State Curving Without Flange Force

FIGURE 9. COMPENSATING GUIDED STEERING TRUCK

$$y = \frac{r_o \ell}{\alpha R} \quad , \quad \psi = 0 \quad , \quad \phi_1 = \phi_2 = 0 \tag{47}$$

The creep forces are zero and the axles are aligned radially, leading to the same solution for the creep guidance region as for the ideal guided steering truck, equation (38).

The truck will reach the high rail when $y_1 = q$, which produces a radius

$$R < \frac{r_o \ell}{\alpha \left(q + \frac{P}{4f} h\ell\right)}, \tag{48}$$

for the truck to remain at the high rail. In order for the truck to traverse the curve at the high rail with <u>zero flange force</u> while maintaining force and moment equilibrium, it is necessary for the angle ϕ to be set correctly. Following Figure 9, for balance speed conditions, the oversteered condition required for steady state curving of the truck without flange force is

$$\phi_1 = - \frac{f_T}{f_L h} \left[\frac{\alpha q}{r_o} - \frac{\ell}{R}\right] , \quad \phi_2 = \phi_1 \quad \psi = 0 . \tag{49}$$

For the case of equal creep coefficients in the lateral and tangential directions, this oversteering condition is equivalent to the oversteering condition required by the ideal radial truck for curving without flange force (31).

The wheel/rail forces on the truck build up as the radius of the curve decreases. The resultant saturation force is oriented in the direction of the resultant creep force. As shown in Figure 7b this orientation is independent of radius and is defined by

$$\tan\beta = \frac{f_T}{h f_L} , \quad \tan\gamma = \tan\beta . \tag{50}$$

The lateral wheel/rail force on the wheels of the leading and trailing axles is

$$\text{Lateral W/R Force} = \mu N \sin\beta \,. \tag{51}$$

For the case with equal lateral and tangential creep coefficient, this lateral component of the saturation force is $.58\mu N$.

7. NUMERICAL RESULTS

A comparison of the wheel/rail forces and the flange force for all five trucks in steady state curving is shown in Figures 8 and 10 at balance speed conditions. These results are based upon the dimensions of a high conicity transit truck with the parameters

$$\alpha = .2,\ q = .405'',\ r_o = 15'',\ \ell = 28.2'',\ h = 1.41,\ P = 0,\ \mu = 0.5,\ W = 100{,}000^{\#} \tag{52}$$

In order to derive first order values for the forces, an estimate of the creep coefficient is needed. An approximate value for the creep coefficient in the linear range is about 150 times the wheel load. Since we are dealing with large creep, a value of about 75 times the normal force is probably more appropriate. The creep coefficient, assuming a 100,000# car weight with two trucks and an equal weight distribution, is then

$$f = \frac{75W}{8} = 9.375 \times 10^5\ \#. \tag{53}$$

It should be emphasized that the results presented in this work are limiting values based on the assumption of sliding of the wheels on both the leading and trailing axles, along with the assumption of flanging on the lead outer wheel. Although other analytical assumptions could lead to more refined results, particularly with respect to variation of force levels with radius in the force saturation region, the results are an upper bound to the force levels for trucks in steady state curving on track without any irregularities. It also should be noted that the trucks analyzed in this report have a dynamic instability characterized by zero critical speed. However, the results of this analysis will enable designers to establish parameters for minimization of curving forces. Design choices involving tradeoffs between curving forces and dynamic stability are addressed in Reference [2].

The lateral lead axle wheel/rail forces are shown in Figures 10 and 11. Except for the compensating guided steering truck and the ideal radial truck, the <u>limiting sliding</u> values of the wheel/rail forces are within 10 percent of 0.9 μN on the low rail and within 5 percent of 1.8 μN on the high rail. The compensating guided steering truck and ideal radial truck, which traverse the curve without flanging by adopting an oversteering orientation have limiting sliding forces of 0.58μN on both the high and low rail. The variation of force with curve radius can be quite different even for trucks that are fairly similar in limiting lateral force levels. For example, for the rigid truck, wheel/rail forces are required for negotiation of all curve radii. For the creep guidance range (no flange contact) these wheel/rail forces are proportional to curvature (1/R), and the angle of attack is zero. Flange contact occurs at 1304 feet. In contrast, the wheel/rail forces for the guided steering trucks are zero in the creep guidance range since the axles align themselves radially and contact with the high rail does not occur until 435 feet. For any truck, the total wheel/rail force is composed of the flange force and the lateral component of the saturation force, μN. This saturation force for the rigid truck acts in a direction more normal (80°) to the rail than for the guided steering truck

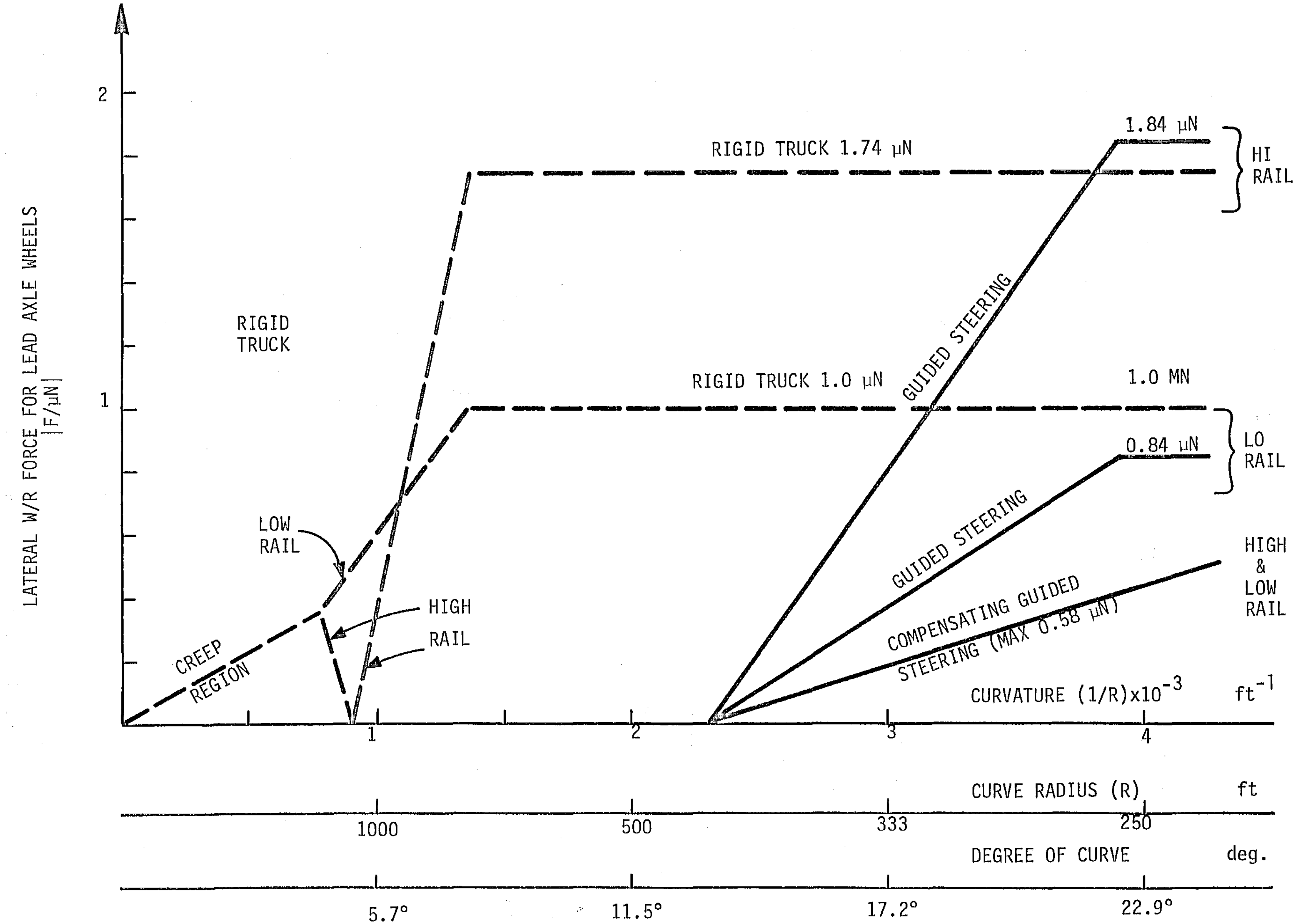

FIGURE 10. LATERAL W/R FORCE ON LEAD AXLE OF RIGID, GUIDED STEERING, AND COMPENSATING GUIDED STEERING TRUCKS (α=0.2, P=0, f=75N)

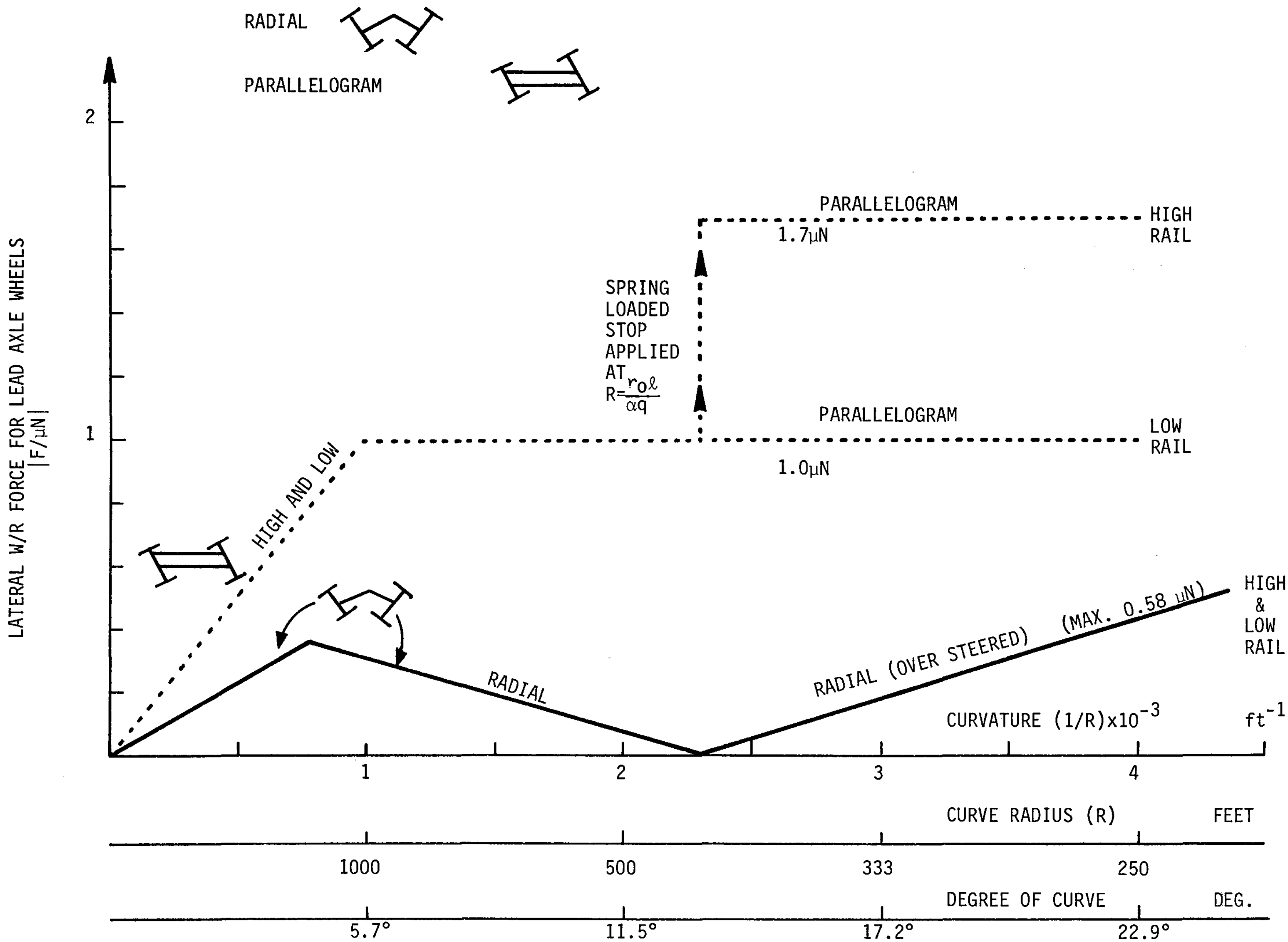

FIGURE 11. LATERAL W/R FORCE ON LEAD AXLE OF RADIAL AND PARALLELOGRAM TRUCKS (α=0.2, P=0, f=75N)

(57°) or for the compensating truck (35°).

For the radial truck (Figure 11), the creep region is identical to that of the rigid truck, as the bending spring K_{ψ} does not deform. The high rail is reached at the same radius of 1304 feet. For smaller curve radius the ideal radial truck moves along the high rail and offsets the increasing track curvature by orienting the axles to an oversteered position. Force saturation for the ideal radial truck occurs at 217 feet (same as for the compensating guided steering truck).

The parallelogram truck (Figure 11) flanges at the mildest curvature of any of the trucks studied, namely tangent track. The buildup of wheel/rail force with curvature is somewhat slower than for the rigid truck with force saturation reached at about 1000 feet with a limiting lateral wheel/rail force of 1.0 μN. For R<435 feet, when the spring loaded stops are applied, the limiting wheel/rail force rises to 1.7 μN due to the greater interaction of the trailing and leading axle.

The limiting flange force for the various trucks is shown in Figure 12. In terms of minimizing flange force, the compensating guided steering truck and the ideal radial truck are obviously best since curve traversal is possible without flange force. The remaining trucks all reach about the same limiting flange force of 2.7 μN. However, the curve radius at which these flange force levels are reached can be quite different as is the rate at which the flange force buildup occurs. For example, the guided steering truck besides traversing a curve three times sharper than for the radial truck without flanging (435 feet vs 1304 feet) also

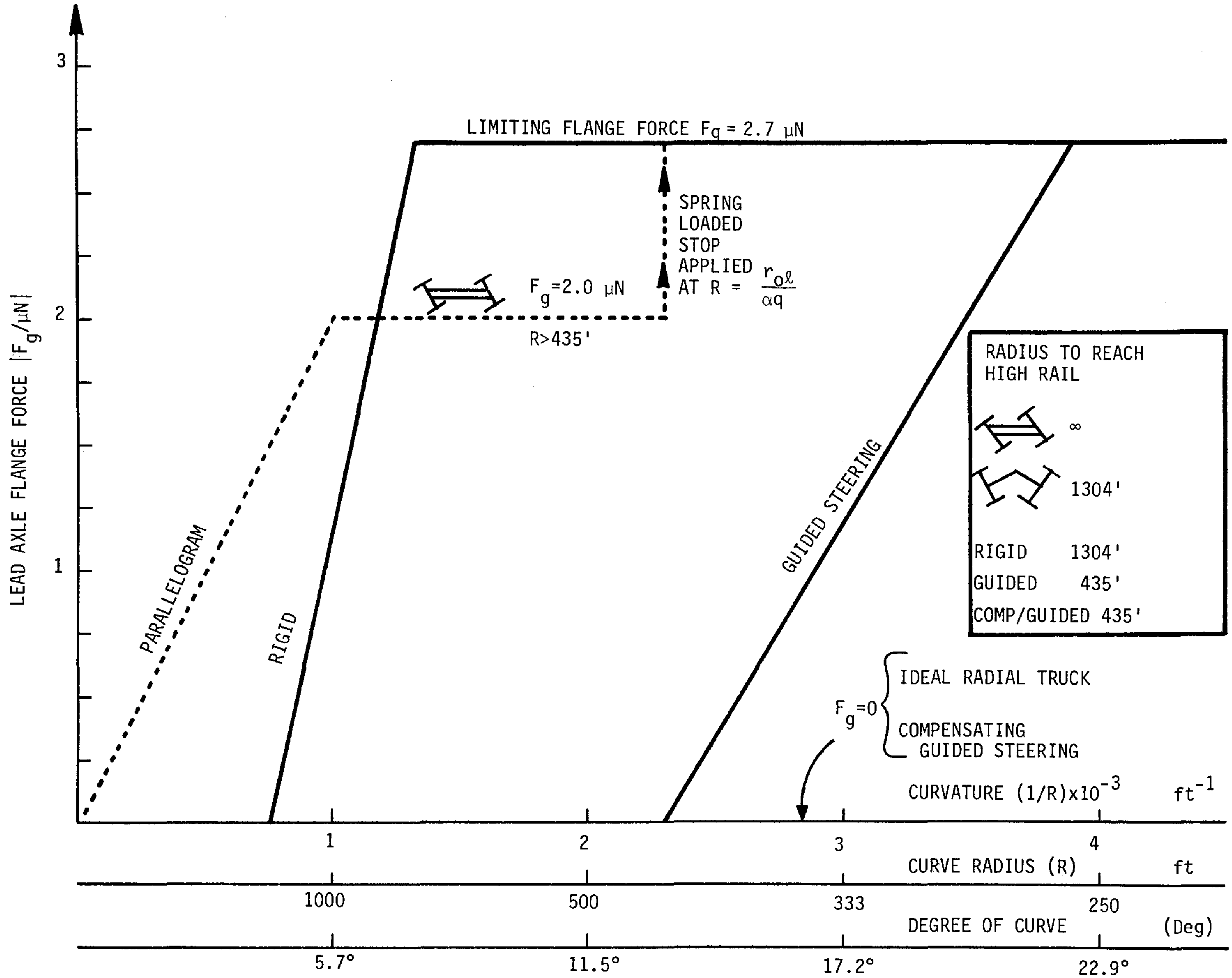

FIGURE 12. FLANGE FORCE (α=.2, P=0, f=75N)

builds up flange force at a slower rate. The rate of increase of flange force with curvature for the guided steering truck is 1/3 the rate for the rigid truck (due to the $(1+h^2)$ factor in the equations). The saturation radius for the rigid truck is about 750 feet versus 250 feet for the guided steering truck. Although the guided steering truck can traverse curves without flanging for radii one-third that for the rigid truck, once flanging takes place both trucks will eventually reach about the same limiting flange force. The effect of conicity on flange force and W/R force is given in Table 1 and the rigid truck appears to be relatively insensitive to conicity effects. However, for cylindrical wheels (α=o), the rigid truck (and the guided steering truck) flanges for all values of curve radius.

The parallelogram truck flanges for all track curvatures, including tangent track. The flange force builds up linearly with curvature until saturation occurs at 1000 feet, with a limiting flange force value of 2.0 μN. For radii sharper than 435', which is the value at which the trailing axle flange clearance is taken up, the truck will collapse unless spring loaded stops are used to maintain static stability. This causes greater interaction between the trailing and leading axles, leading to an increase of flange force with a limiting value of 2.7 μN.

TABLE 1. LEAD-AXLE LATERAL-SATURATION FORCES FOR RIGID TRUCK

	RIGID TRUCK FORCES	
Wheel Taper	$\alpha = 0$	$\alpha = .2$
Flange Force	$2.76\mu N$	$2.74\mu N$
Hi Rail W/R Force	$1.80\mu N$	$1.74\mu N$
Lo Rail W/R Force	$0.96\mu N$	$1.0\ \mu N$
Curve Radius at Saturation (μ=0.5)	1095	750 feet
Curve Radius at Flange Contact	All	1304 feet

CONCLUSIONS

This work presents techniques and solutions for predicting bounds for wheel/rail forces and flange forces for several types of rigid and flexible trucks in steady state curving conditions. The analysis provides closed form relations for estimating forces, truck angle of attack and sliding conditions as a function of truck geometry and track parameters. Limiting case transit truck configurations are analyzed and compared to provide an estimate of the benefits in curving performance that can be achieved by modifying truck geometry and parameters. These limiting configurations include:

1. Ideal rigid truck
2. Ideal parallelogramming truck
3. Ideal radial (self steering) truck
4. Ideal guided steering truck
5. Compensating guided steering truck

For the parameters used in the numerical study, the following relative comparisons can be made between the trucks analyzed:

i) Only the two types of guided steering trucks analyzed are capable of steady state curving without wheel/rail force (R>435 ft).

ii) In terms of <u>limiting wheel/rail force</u> on the high rail for R<435 feet, the rigid, parallelogram and guided steering trucks produce about the same force levels. The compensating guided steering truck and ideal radial truck have a limiting wheel/rail force on the high rail factor of three <u>less</u> than the values of the other trucks. For R>435 feet, the parallelogram truck has a maximum value 40% less than its limiting wheel/rail force for R<435'.

iii) In terms of limiting flange force the trucks produce about the same force level, except for the compensating guided steering truck and ideal radial truck which traverse the curve without flanging by adopting an oversteered position. For R>435 feet, the parallelogram truck has a maximum value 37% less than its limiting flange force for R<435 feet.

iv) In terms of track curvature that the trucks can traverse without force saturation occurring, the trucks can be ranked from lowest to highest curvature as parallelogram, rigid, guided steering, compensating guided steering, and radial. The parallelogram truck reaches a radius of about 1000 feet when saturation occurs, whereas the compensating guided steering truck and ideal radial truck can traverse a radius as low as 217 feet before force saturation occurs.

These results and comparisons are typical of the design uses of the tools developed in this work. Design choices involving trade-offs between curving performance and dynamic stability considerations are also useful and some details are given in Reference [2].

REFERENCES

1. Weinstock, H. and Greif, R., "Analysis of Wheel/Rail Force and Flange Force During Steady-State Curving of Rigid Trucks," DOT-TSC-UMTA-80-26, UMTA-MA-06-0025-80-8, Interim Report, September 1980. (Also ASME Paper No. 81-RT-5, presented at the Joint ASME/IEEE Railroad Conference, April 1981.)
2. Bell, C.E., Horak D., and Hedrick, J.K., "Stability and Curving Mechanics of Rail Vehicles," ASME Paper No. 80-WA/DSC-15, presented at Winter Annual Meeting of ASME, November 1980.

APPENDIX A

ALTERNATIVE CALCULATION OF MAXIMUM FORCES FOR RIGID TRUCK

In the body of this report, the investigation of the limiting force levels on the wheels of the lead axle is done with the assumption of slipping of both the front and back wheels in the free curving region. The resulting calculation (e.g., equations (9) and (10)) is somewhat tedious due to the dependence of yaw angle on curve radius. A simpler approach is to assume the rigid truck is in the constrained curving region (which fixes ψ as a constant) and then use an asymptotic analysis for small R. In this Appendix, the rigid truck will be analyzed in this manner and it will be shown that the value of the flange force is less than that found from equations (9) and (10) associated with the free curving region.

For the constrained region, it follows from (7)

$$\psi = q/h\ell . \tag{A-1}$$

Considering Figure 2 with a flange force acting on the trailing axle at the low rail leads to the following equilibrium relations,

$$\sum F: \quad F_{g_1} - F_{g_2} = 2\mu N \sin\beta + 2\mu N \sin\gamma,$$

$$\sum M: \quad F_{g_2} = -\, 2\mu N \sin\gamma + \frac{\mu N}{h}(\cos\beta + \cos\gamma). \tag{A-2}$$

The trigonometric terms, and the associated asymptotic values for small R, are

$$\sin\beta = \frac{h\ell/R + \psi}{\sqrt{\left(\frac{h\ell}{R} + \psi\right)^2 + \left(\frac{\ell}{R} - \frac{\alpha q}{r_o}\right)^2}},$$

$$\sin\beta \sim \frac{h}{\sqrt{1 + h^2}}, \quad \cos\beta \sim \frac{1}{\sqrt{1 + h^2}} \tag{A-3}$$

$$\sin\gamma = \frac{\frac{h\ell}{R} - \psi}{\sqrt{\left(\frac{h\ell}{R} - \psi\right)^2 + \left(\frac{\ell}{R} - \frac{\alpha}{r_o}\left\{q - 2h\ell\psi\right\}\right)^2}},$$

$$\sin\gamma \sim \frac{h}{\sqrt{1 + h^2}}, \quad \cos\gamma \sim \frac{1}{\sqrt{1 + h^2}}.$$

Substituting these relations into (A-2) leads to the following limiting value of flange force,

$$F_{g_1} = 2\mu N \sin\beta + \frac{\mu N}{h} (\cos\beta + \cos\gamma)$$

$$\sim \frac{2\mu N}{h} \sqrt{1 + h^2}$$

$$\sim 2.45\mu N$$

This limit is less than the value of $2.74\mu N$ obtained from free curving assumptions analyzed in the text. Further analysis of limiting values can be done from the equations derived in this Appendix by parametrically letting the radius R increase in value while maintaining ψ as constant.

APPENDIX B

PARALLELOGRAM TRUCK: MINIMUM STIFFNESS REQUIRED TO MAINTAIN EQUILIBRIUM FOR FREE-CURVING REGIME

As discussed in Section 3, the parallelogram truck with pinned connections can maintain static equilibrium as long as the trailing axle flange clearance is not taken up, i.e., $R > r_o\ell/\alpha q$. For sharper curves, $R < r_o\ell/\alpha q$, spring loaded stops (modelled as torsional springs) must be used to maintain stability in the free curving region. The PVW can be used to verify and derive equilibrium and stability conditions.

Consider the parallelogram truck shown in Figure (B-1) at a warping angle Φ and yaw angle ψ^* with creep forces acting. The yaw angle ψ^* is defined as the deviation from the yaw angle $h\ell/R$ which the axles attain when both axles are at the high rail, as defined by equation (19). The warping angle Φ is defined as the deviation in warping angle from that attained when both axles are at the high rail. Arbitrary virtual displacements $\delta\Phi$ and $\delta\psi^*$ are considered from the equilibrium position of the truck in free curving (i.e., for these purposes, the truck is considered pinned to the high rail at A). The IVW done by the torsional springs through $\delta\Phi$ is

$$IVW = (4K\Phi)\delta\Phi\ , \tag{B-1}$$

and the EVW done by the creep forces through $\delta\Phi$ and $\delta\psi^*$ is

$$EVW = -\ (2f\psi^*)(2h\ell)(\delta\Phi + \delta\psi^*)$$
$$+\ 2f\ell\left(\frac{\ell}{R} - \frac{\alpha}{r_o}\, y_2\right)\delta\psi^* + 2f\ell\left(\frac{\ell}{R} - \frac{\alpha}{r_o}\, q\right)\delta\psi^*\ . \tag{B-2}$$

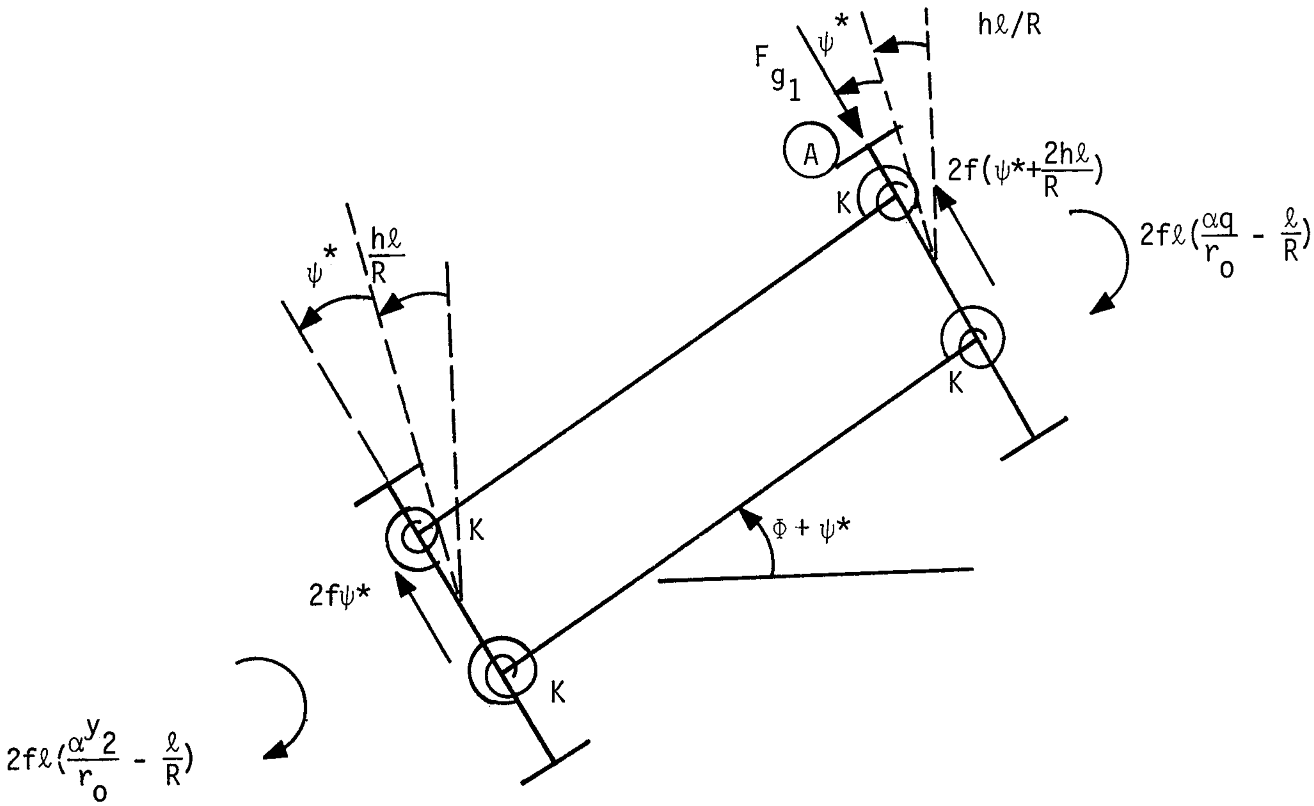

FIGURE B-1. CREEP FORCES ACTING ON PARALLELOGRAM TRUCK WITH SPRING-LOADED STOPS

Equating IVW to the EVW leads to

$$4(K\Phi + h\ell f\psi^*)\delta\Phi - 2f\ell\left(\frac{2\ell}{R} - \frac{\alpha}{r_o}\left\{y_2 + q\right\} - 2h\psi^*\right)\delta\psi^* = 0. \quad \text{(B-3)}$$

Since the virtual displacements are arbitrary, it follows that each term in parentheses must vanish. The first term produces

$$\Phi = -\frac{h\ell f}{K}\psi^* . \quad \text{(B-4a)}$$

This relationship can be used to define the minimum spring stiffness required for stability in the free curving regime. For the parallelogram truck in free curving, the position of the rear axle, y_2, in terms of the lead axle can be written as

$$\begin{aligned} y_2 &= q - 2h\ell(\Phi + \psi^*), \\ y_{2_{max}} &= q \quad \text{(at high rail).} \end{aligned} \quad \text{(B-4b)}$$

By substituting the relationship between warping angle Φ and yaw angle ψ^* from (B-4a) into (B-4b), the minimum stiffness K for the torsional springs is found to be

$$K \geq fh\ell \quad \text{(B-5)}$$

The equilibrium relation defining the yaw angle ψ^* is obtained by setting the second parenthesis in (B-3) to zero

$$y_2 = -q + \frac{2r_o}{\alpha}\left(\frac{\ell}{R} - h\psi^*\right), \quad \text{(B-6)}$$

and then using (B-4a), and (B-4b),

$$\psi^* = \frac{\ell/R - \alpha q/r_o}{h\left(1 - \frac{\alpha\ell}{r_o} + \frac{\alpha\ell}{r_o}\frac{fh\ell}{K}\right)} \quad (\alpha\ell/r_o < 1). \quad \text{(B-7)}$$

106 Copies